CRYSTAL GROWTH & DESIGN

Article

pubs.acs.org/crystal

Anion−Anion Interactions in the Crystal Packing of Functionalized Methanide Anions: An Experimental and Computational Study

Anthony S. R. Chesman,[†,‡] Jennifer L. Hodgson,[†] Ekaterina I. Izgorodina,*[,†] Aron Urbatsch,[†] David R. Turner,[†] Glen B. Deacon,[†] and Stuart R. Batten*[,†]

[†]School of Chemistry, Monash University, Wellington Road, Clayton, Victoria 3800, Australia

[‡]CSIRO Materials Science and Engineering, Bayview Avenue, Clayton, Victoria 3168, Australia

Supporting Information

ABSTRACT: Examination of the crystal structures of $(Me_4N)(dcnm)$ (**1**), $(Me_4N)(dcnom)$ (**2**), and (Me_4N)-(nbdm) (**3**) [dcnm = dicyanonitrosomethanide, dcnom = dicyanonitromethanide, nbdm = nitroso-*N*,*N*-bis-(dicyanomethanide)] reveals the anions pack in an unusual columnar array, with distances between the planar species suggestive of $\pi-\pi$ stacking. This columar packing motif is not observed in the crystal structures of $(Me_4N)(ccnm)$ (**4**) and $(Me_4N)(ccnom)$ (**6**) (ccnm = carbamoylcyanonitrosomethanide, ccnom = carbamoylcyanonitromethanide), in which hydrogen bonding between anions is the dominant supramolecular interaction. Ab initio calculations performed at the HF and MP2 levels of theory on ionic clusters of varying size further explored the nature and strength of anionic interactions observed in crystal structures. The first syntheses of the nbdm and ccnom anions are also reported.

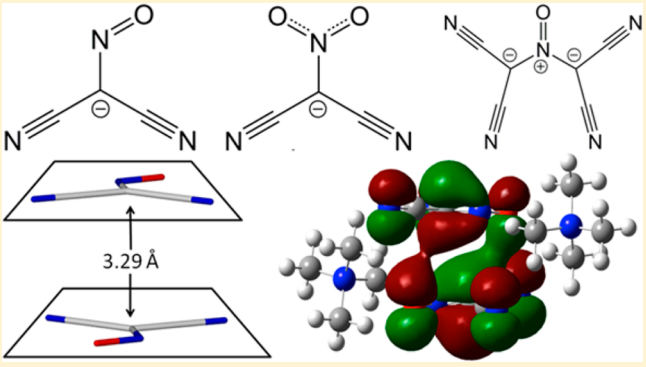

INTRODUCTION

One of the earliest principles taught to students of chemistry is that electrostatic forces will cause oppositely charged species to attract each other, while like-charged species will be repelled. Therefore, in the crystal structure of ionic systems, anions and cations will pack in a fashion that minimizes their interatomic distance, while electrostatic repulsion will maximize the space between like-charged species. As a consequence, in simple crystal systems containing similarly sized ions such as NaF, it is expected that anions will be adjacent only to cations and vice versa. However, this simplified rule for predicting crystal packing does not hold for all ionic systems, and intermolecular distances less than the sum of the van der Waals radii of like-charged ions may arise due to either packing constraints caused by a size or shape disparity between ions or additional attractive intermolecular interactions, which stabilize the system.[1]

Anion−anion interactions have been observed to occur in numerous systems, including between polyiodide species,[2] nitrate anions,[3] phthalocyanines,[4] the halide component of rock salts and hydroxyammonium chloride,[5] nitroprusside metal complexes,[6] and in hydrogen bonding systems.[7] A reoccurring motif in anion−anion interactions is the formation of π stacked columns, most frequently seen in crystal structures containing TCNQ (7,7,8,8-tetracyano-*p*-quinodimethane) and TCNE (tetracyanoethylene) radical anions.[8] This packing motif may persist in a broad variety of chemical environments, which feature additional intra- and intermolecular interactions of varying strength.[9] The columns have also been observed in crystal structures of neutral metal complexes that incorporate $\kappa^1(C{\equiv}N)$ coordinating ligands,[10] in alkali metal salts of the anions,[11] and organic salts with hydrogen bonding and $\pi-\pi$ stacking cations.[12] Columns of planar anions also occur in crystal structures of metal complexes containing the maleonitriledithiolate (mnt) ligand.[13] The relative position of anions within columns is critical to mediating the magnetic interaction between adjacent metal centers,[14] a relationship that also extends to discrete $[M(mnt)_2]^-$ dimers.[15]

Our own research in recent years has focused on a group of pseudohalides that consists of methanide anions functionalized with carbamoyl, nitrile, nitroso, and nitro groups (Scheme 1).[16] These electron-withdrawing functional groups delocalize the negative charge over the anion, resulting in highly stable, planar species. To date, these methanides have been included in a broad range of applications, including ionic liquids (ILs),[16c,17] photovoltaic devices,[18] cytotoxic compounds,[19] magnetic materials,[20] gas-sensing frameworks,[21] and energetic materials.[22] The dicyanonitrosomethanide (dcnm) anion is of particular interest, as it has the propensity to undergo the addition of a nucleophile to a nitrile group.[23] This has been exploited with the in situ synthesis of ligands with diverse coordination modes that are incorporated into magnetically active coordination polymers and clusters.[16a,24] The nitroso

Received: January 9, 2014
Revised: February 19, 2014
Published: February 21, 2014

Scheme 1. Molecular Structure of Dicyanonitrosomethanide (dcnm), Dicyanonitromethanide (dcnom), Carbamoyldicyanomethanide (cdm), Cyanonitronitrosomethanide (cnnom), Trinitromethanide (tnom), and Cyanodinitromethanide (cdnom)

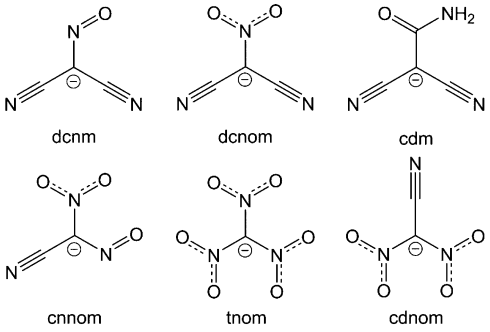

group of the dcnm anion may also react to form oximate bridges.[25]

The organic salts of the carbamoyldicyanomethanide anion have been broadly studied for their ability to form a variety of anionic hydrogen-bonded networks, with engineering of the hydrogen-bonding motifs present within the crystal structure made possible by the judicial selection of counter-cation.[26] However, the supramolecular chemistry of the other organic methanide salts remains relatively unexamined, despite the fact their unique electronic structure may offer insights into supramolecular interactions between anions.

Herein, we report the first syntheses of the new anions nitroso-*N*,*N*-bis(dicyanomethanide) (nbdm) and carbamoylcyanonitromethanide (ccnom). We have investigated the columnar packing of anions that arise from unusual anion−anion interactions, observed in the crystal structures of tetramethylammonium salts of the polynitrile methanides dcnm (**1**), dcnom (**2**), and nbdm (**3**). We have also studied the analogous tetramethylammonium salts of methanides with carbamoyl functional groups, ccnm (**4**) and ccnom (**5**), and consider the effects that the dominant hydrogen-bonding interactions have on the crystal structures of these species. The strength and origin of the specific interactions were also explored through a series of quantum chemical calculations performed at a highly correlated level of theory.

EXPERIMENTAL SECTION

Materials. All materials and solvents were purchased from standard commercial sources and used without further purification. Ag(dcnm),[27] Ag(dcnom),[28] Ag(ccnm),[24c] (Me_4N)(dcnm) (**1**), and (Me_4N)(ccnm) (**4**)[23c] were prepared by literature methods. Crystals of **1** suitable for X-ray crystallography were grown by the diffusion of diethyl ether into a dilute solution of **1** dissolved in acetone.

Instrumentation. Infrared data were collected using a Perkin-Elmer ATR−FTIR spectrometer in the range of 4000−500 cm^{-1} with a resolution of 4 cm^{-1}. Elemental analyses were performed by the Campbell Microanalytical Laboratory of the University of Otago, New Zealand. Mass spectrometry was performed on a Micromass Platform 2 mass spectrometer with an electrospray source and a variable cone voltage with samples dissolved in methanol or dimethyl sulfoxide. ^{13}C NMR spectra were recorded in D_2O or DMSO-d_6 on a Bruker Avance 400 (9.4 T magnet) with a 5 mm broadband autotunable probe with *Z* gradients and a BACS 60 tube autosampler. Differential scanning calorimetry (DSC) experiments were conducted using a ThermalAnalysis DSC Q100, and data were analyzed using Universal Analysis 2000 V4.1D, Build 4.1.0.16 software. Samples were heated and cooled at a rate of 10 °C/min and held at the respective minimum/maximum temperature for 3 min before cooling/heating for the second cycle.

Synthesis. (Me_4N)(dcnom) (**2**) (dcnom = dicyanonitromethanide): Ag(dcnom) (1.979 g, 9.081 mmol) was added to (Me_4N)Cl (0.995 g, 9.078 mmol) dissolved in methanol (30 mL). The solution was covered from light and stirred for one hour, resulting in the formation of a precipitate of AgCl. The solution was filtered to remove the precipitate, and the solvent was evaporated under reduced pressure to yield an orange solid. This solid was suspended in methanol (25 mL) and heated at reflux for two hours while covered from light. The solution was filtered to remove a white precipitate, which did not dissolve in the methanol. The filtrate was stored at −18 °C for one week, yielding orange needle crystals of the product. The crystals were filtered from the reaction solution, washed with cold methanol, and dried under vacuum for two hours (0.775 g, 46%). The filtrate was retained for the isolation of crystals of (Me_4N)(nbdm) (**3**) (see below). As **2** is hygroscopic, a sample was submitted for elemental analysis in a sealed ampule under an atmosphere of nitrogen. IR (ATR): ν = 3480 (vw), 3041 (w), 2204 (s), 2190 (s), 1481 (s), 1421 (sh), 1402 (m), 1320 (vs), 1284 (sh), 1157 (m), 948 (m), 746 (w) cm^{-1}. ^{13}C NMR (100.6 MHz, DMSO-d_6): δ = 54.4 (Me_4N^+), 76.5 (C−NO_2), 115.1 (C≡N). Elemental analysis calcd (%) for $C_7H_{12}N_4O_2$ (184.20): C, 45.64; H, 6.57; N, 30.42. Found: C, 45.74; H, 6.68; N, 30.58.

(Me_4N)(nbdm) (**3**) [nbdm = nitroso-*N*,*N*-bis(dicyanomethanide)]: The filtrate from the synthesis of (Me_4N)(dcnom) (**2**) was allowed to evaporate slowly to dryness. Among the amorphous precipitate of (Me_4N)(dcnom), which had failed to crystallize from the evaporating reaction solution, were distinct orange needle crystals of (Me_4N)(ndbm). These crystals of (Me_4N)(nbdm) were manually separated from the precipitate with no further treatment (5 mg). IR (ATR): ν = 3039 (w), 2200 (s), 1609 (w), 1483 (m), 1395 (m), 1364 (m), 1246 (w), 1213 (w), 946 (m), 880 (w), 671 (w) cm^{-1}. ESI-MS^+: m/z = 73.8 (Me_4N^+, 100%). ESI-MS^-: m/z = 157.8 ($nbdm^-$, 100%). Elemental analysis calcd (%) for $C_{10}H_{12}N_6O$ (232.24): C, 51.72; H, 5.21; N, 36.20. Found: C, 51.76; H, 5.53; N, 35.93.

Ag(ccnom) (**5**) (ccnom = carbamoylcyanonitromethanide): NaCl (1.06 g, 18.14 mmol) was added to Ag(ccnm) (4.35 g, 19.78 mmol) suspended in methanol (50 mL). Water (50 mL) was added to the reaction solution, which was then covered from light and vigorously stirred for one hour, resulting in the formation of a white precipitate of AgCl. The AgCl and remaining unreacted Ag(ccnm) were filtered from the reaction solution, leaving a yellow filtrate. The solvent was removed under reduced pressure, leaving Na(ccnm) as a light yellow solid (2.25 g, 92%). This product was dissolved in acetic acid (40 mL) and water (20 mL). $(NH_4)_2[Ce(NO_3)_6]$ (18.23 g, 33.25 mmol) dissolved in water (100 mL) was slowly added to the reaction solution, causing the light yellow solution to change to a deep red color. The solution was stirred for one hour, during which time the color of the solution changed to light orange. $Ag(NO_3)$ (3.26 g, 19.18 mmol) dissolved in water (40 mL) was added to the reaction solution, resulting in the formation of a light orange precipitate, which was filtered from the reaction solution and washed with ethanol and diethyl ether

dx.doi.org/10.1021/cg500051m | *Cryst. Growth Des.* 2014, 14, 1922−1932

(1.70 g). The solvent was removed from the filtrate under reduced pressure until the volume was approximately 20 mL, and the solution was stored at 4 °C, yielding the first crop of crystals. The aforementioned light orange precipitate was suspended in water (300 mL) and heated under reflux for six hours. The remaining suspension was then filtered off and discarded, while the filtrate was stored at 4 °C to yield a second crop of crystals. Both crops of crystals were collected, combined together, washed with ethanol and diethyl ether, and dried under vacuum for one hour. IR (ATR): ν = 3372 (s), 3257 (w), 3179 (s), 2196 (m), 1646 (s), 1545 (m), 1466 (m), 1329 (m), 1227 (w), 1139 (w), 1071 (w), 752 (w), 694 (w) cm^{-1}. ESI-MS^-: m/z = 85.0 ($C_3H_5N_2O^-$, 50%), 128.0 (ccnom$^-$, 100%), 363.0, 364.8 ([Ag(ccnom)$_2$]$^-$, 30%). ^{13}C NMR (100.6 MHz, DMSO-d_6): δ = 97.8 (C−NO_2), 118.6 (C≡N), 163.7 ($CONH_2$). Elemental analysis calcd (%) for $C_3H_2AgN_3O_3$ (235.93): C, 15.27; H, 0.85; N, 17.81. Found: C, 15.49; H, 1.00; N, 17.80.

(Me_4N)(ccnom) (**6**): Ag (ccnom) (**5**) (285 mg, 1.207 mmol) was suspended in methanol (7 mL) and sonicated for several minutes to break the crystals down to a fine powder. (Me_4N)Cl (132 mg, 1.204 mmol) was added to the reaction solution, resulting in the formation of a light white precipitate of AgCl. The reaction solution was covered from light and stirred for one hour, resulting in further precipitation of AgCl from the solution. The AgCl was filtered from the reaction solution. Under reduced pressure, the volume of the filtrate was reduced to 3 mL. Diethyl ether (1 mL) was added to the solution, which was then stored at −18 °C, with a large crystal forming from the solution within 24 h. This very lightly orange-colored crystal of (Me_4N)(ccnom) was filtered from the reaction solution, washed with cold ethanol and diethyl ether, and dried under vacuum for one hour (75 mg, 31%). As the material is hygroscopic, a sample was submitted for elemental analysis in a sealed ampule under an atmosphere of nitrogen. IR (ATR): ν = 3383 (m), 3292 (w), 3152 (m), 3035 (w), 2196 (m), 1637 (m), 1558 (w), 1488 (m), 1445 (m), 1330 (s), 1212 (w), 1132 (m), 1083 (w), 947 (m), 791 (w), 761 (w), 689 (w), 616 (w) cm^{-1}. ^{13}C NMR (100.6 MHz, DMSO-d_6): δ = 54.4 (Me_4N^+), 97.9 (C−NO_2), 117.9 (C≡N), 163.7 ($CONH_2$). ESI-MS^+: m/z = 74.0 (Me_4N^+, 100%); 276.2 ([(Me_4N)$_2$(ccnom)]$^-$, 20%), ESI-MS^-: m/z = 85.0 ($C_3H_5N_2O^-$, 50%), 128.0 (ccnom$^-$, 100%). Elemental analysis calcd (%) for $C_7H_{14}N_4O_3$ (202.21): C, 41.58; H, 6.98; N, 27.71. Found: C, 41.70; H, 7.19; N, 27.48.

X-ray Crystallography. Crystals were mounted on fine glass fibers using viscous hydrocarbon oil. Data were collected on Bruker X8 Apex II CCD (**2**, **3**, **6**) or Nonius Kappa-CCD (**1**, **5**) diffractometers, both equipped with graphite monochromated Mo Kα radiation (λ = 0.71073 Å). Data collection temperatures were maintained at 123 K using an open flow N_2 cryostream. Solutions were obtained by direct methods or Patterson synthesis using SHELXS 97[29] followed by successive refinements using full matrix least-squares method against F^2 using SHELXL 97.[29] The program X-Seed was used as a graphical SHELX interface.[30] For data collected on the Nonius KappaCCD diffractometer, integration was carried out by the program DENZO-SMN and data were corrected for Lorentz-polarization effects and for absorption using the program SCALEPACK.[31] For data collected on the Bruker X8 Apex II diffractometer integration was carried out by the program SAINT using the Apex II software suite.[32] All data sets were treated for the effects of absorption. CCDC 980519 (**1**), CCDC 980520 (**2**), CCDC 980521 (**3**), CCDC 980522 (**5**), and CCDC 980523 (**6**) contain the supplementary crystallographic data for this paper. These data can be obtained free of charge from the Cambridge Crystallographic Data Centre at www.ccdc.cam.ac.uk/data_request/cif.

X-ray Crystal Data. (Me_4N)(dcnm) (**1**): $C_7H_{12}N_4O$, M = 168.21, yellow needle, 0.30 × 0.20 × 0.10 mm^3, monoclinic, space group $P2_1/m$ (no. 11), a = 8.6630(17), b = 6.5838(13), c = 9.0253(18) Å, β = 116.56(3)°, V = 460.4(2) Å^3, Z = 2, D_c = 1.213 g/cm^3, F_{000} = 180, μ = 0.086 mm^{-1}, $2\theta_{max}$ = 55.0°, 3128 reflections collected, 1137 unique (R_{int} = 0.0606). Final *GooF* = 1.140, *R*1 = 0.0691, *wR*2 = 0.1782, *R* indices based on 879 reflections with $I > 2\sigma(I)$ (refinement on F^2), 86 parameters, 0 restraints. The nitroso group of the dcnm ligand is disordered over two positions with the occupancy of the sites allowed to refine against each other (69:31).

(Me_4N)(dcnom) (**2**): $C_7H_{12}N_4O_2$, M = 184.21, colorless block, 0.20 × 0.20 × 0.10 mm^3, monoclinic, space group $P2_1/c$ (no. 14), a = 11.5852(12), b = 15.6154(19), c = 11.3954(11) Å, β = 109.555(5)°, V = 1942.6(4) Å^3, Z = 8, D_c = 1.260 g/cm^3, F_{000} = 784, μ = 0.095 mm^{-1}, $2\theta_{max}$ = 55.0°, 15447 reflections collected, 4453 unique (R_{int} = 0.0318). Final *GooF* = 1.046, *R*1 = 0.0463, *wR*2 = 0.1161, *R* indices based on 3251 reflections with $I > 2\sigma(I)$ (refinement on F^2), 243 parameters, 0 restraints.

(Me_4N)(nbdm) (**3**): $C_{10}H_{12}N_6O$, M = 232.26, yellow needle, 0.20 × 0.07 × 0.04 mm^3, monoclinic, space group $C2/c$ (no. 15), a = 11.5051(8), b = 16.5318(11), c = 6.3634(4) Å, β = 93.046(2)°, V = 1208.61(14) Å^3, Z = 4, D_c = 1.276 g/cm^3, F_{000} = 488, μ = 0.090 mm^{-1}, $2\theta_{max}$ = 50.0°, 2549 reflections collected, 1032 unique (R_{int} = 0.0217). Final *GooF* = 1.098, *R*1 = 0.0519, *wR*2 = 0.1236, *R* indices based on 941 reflections with $I > 2\sigma(I)$ (refinement on F^2), 81 parameters, 0 restraints.

Ag(ccnom) (**5**): $C_3H_2AgN_3O_3$, M = 235.95, light orange needle, 0.20 × 0.10 × 0.10 mm^3, monoclinic, space group $P2_1/c$ (no. 14), a = 3.5082(7), b = 15.467(3), c = 9.6850(19) Å, β = 98.03(3)°, V = 520.38(18) Å^3, Z = 4, D_c = 3.012 g/cm^3, F_{000} = 448, μ = 3.806 mm^{-1}, $2\theta_{max}$ = 55.0°, 4949 reflections collected, 1202 unique (R_{int} = 0.0577). Final *GooF* = 1.075, *R*1 = 0.0256, *wR*2 = 0.0531, *R* indices based on 983 reflections with $I > 2\sigma(I)$ (refinement on F^2), 91 parameters, 0 restraints.

(Me_4N)(ccnom) (**6**): $C_7H_{14}N_4O_3$, M = 202.22, colorless shard, 0.20 × 0.20 × 0.10 mm^3, monoclinic, space group $P2_1/n$ (no. 14), a = 7.4023(3), b = 17.2639(8), c = 8.3753(4) Å, β = 95.899(2)°, V = 1064.63(8) Å^3, Z = 4, D_c = 1.262 g/cm^3, F_{000} = 432, μ = 0.100 mm^{-1}, $2\theta_{max}$ = 55.0°, 8837 reflections collected, 2440 unique (R_{int} = 0.0246). Final *GooF* = 1.059, *R*1 = 0.0362, *wR*2 = 0.0996, *R* indices based on 2020 reflections with $I > 2\sigma(I)$ (refinement on F^2), 131 parameters, 0 restraints.

Theoretical Procedures. Clusters containing one, two, and three ion pairs (IPs) of tetramethylammonium cations coupled with functionalized methanide anions were optimized at the M06-2X[33]/cc-pVDZ[34] level in a solvent field represented by the conductor-like polarizable continuum model (CPCM) method.[35] Ethanol, possessing a dielectric constant similar to that of many ionic liquids,[36] was used as a solvent to adequately treat the stabilization effects imposed by surrounding ions in the bulk. Gas phase geometry optimizations did not produce the neat stacking of methanide anions due to the fact that the gas phase does not favor the electrostatic interactions between charged species. Geometry optimizations were performed with no additional restraints applied. Improved electronic energies of the one-, two- and three-ion paired clusters were obtained using

the fragment molecular orbital approach (FMO)[37] in combination with a second order of Moller−Plesset perturbation theory (MP2)[38] and Ahlrichs TZVPP basis set.[39] The FMO-MP2 method utilized second- and third-body corrections (abbreviated as FMO3-MP2),[40] and the individual ions within were selected as fragments in the approach. Izgorodina et al.[41] validated the use of the FMO3-MP2 method for reliable calculations of energetics in ionic liquid clusters. The same criteria were used as established in our previous work for selecting two- and three-body fragments that need to be included in FMO3-MP2 single-point calculations.[41]

Gas-phase FMO3-MP2 total electronic energies of clusters were computed with the view of deconvoluting interaction energies into two energetic components: electrostatic and dispersion, thus offering an understanding which of these components was responsible for the anion stacking behavior observed in crystal structures. The relative interaction energies of the two- and three ion-paired clusters were calculated with respect to those of single ion pairs, where N is the number of ion pairs in the cluster (i.e., 1, 2, or 3):

$$\Delta E_{\text{int}}(NIP) = \frac{E(NIP)}{N} - E(1IP) \quad (1)$$

where $E(NIP)$ and $E(1IP)$ are FMO3-MP2 electronic energies of the systems consisting of N ion pairs and one ion pair, respectively. The electronic energies in eq 1 were also corrected for the basis set superposition error using the Boys and Bernardi approach.[42] In addition, the relative interaction energy from eq 1 is compared to N individual (i.e., noninteracting) ion pairs and therefore mainly returns stabilization energy due to interactions between anions. Relative interaction energies were calculated at both Hartree−Fock (HF) and MP2 levels of theory. The HF level of theory predominantly recovers Coulomb and induction interactions, whereas any stabilization energy resulting from dispersion forces (e.g., long-range $\pi-\pi$ stacking) is accumulated in the MP2 correlation energy.

The geometry optimization calculations were performed using GAUSSIAN09 (Table S1 of the Supporting Information),[43] whereas the MP2 and FMO3-MP2 calculations were performed using GAMESS-US (Table S2 of the Supporting Information).[44]

RESULTS AND DISCUSSION

Synthesis. For this study, a range of tetramethylammonium salts of functionalized methanide anions and their water addition derivatives were crystallized in order to examine the presence of anion−anion interactions in their crystal structures. (Me_4N)(dcnm) (**1**), (Me_4N)(dcnom) (**2**), and (Me_4N)(ccnm) (**4**) were synthesized by a metathesis between their respective silver salts and tetramethylammonium chloride. Once the resultant insoluble silver halide salt had been removed, the target product was isolated by crystallization from the reaction solution or by removal of the solvent under vacuum, yielding the product as a dry powder, which was recrystallized.

During the synthesis of (Me_4N)(dcnom) (**2**), an unexpected byproduct serendipitously formed. When a filtrate from which crystals of (Me_4N)(dcnom) formed was allowed to slowly evaporate to dryness, several large orange needle crystals deposited among an amorphous precipitate of (Me_4N)(dcnom). These distinct needle crystals were manually isolated and X-ray crystallography revealed the byproduct to be (Me_4N)(nbdm) [nbdm = nitroso-*N*,*N*-bis(dicyanomethanide)] (**3**) (Figure 1). Elemental analysis and mass spectrometry definitively confirmed the composition of the product, with

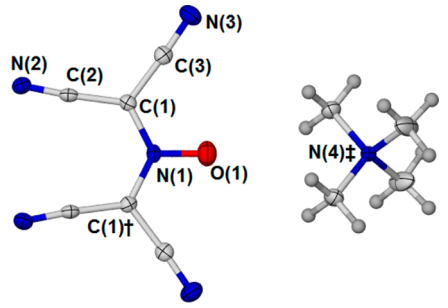

Figure 1. The asymmetric unit in the crystal structure of (Me_4N)(nbdm) (**3**). Ellipsoids shown at 50% probability. Symmetry elements used: † = $-x, y, 1/2 - z$. ‡ = $x - 1/2, 1/2 + y, 1/2 - z$. Selected bond lengths (Å) and angles (deg): N(1)−O(1), 1.266(3); N(1)−C(1), 1.360(2); C(1)−C(2), 1.419(3); C(2)−N(2), 1.151(3); O(1)−N(1)−C(1), 116.7(2); N(1)−C(1)−C(2), 124.7(2).

further characterization restricted due to the prohibitively small amount of material isolated. The low yield of the byproduct and the need for handpicking to isolate the material preclude this synthetic method being a practical route to forming (Me_4N)(nbdm) in useful quantities, with further studies required to develop a high yield synthesis of this unusual anion.

To the best of our knowledge, the nbdm species is yet to be reported and was most likely formed as a minor byproduct during the oxidation of dcnm to the dcnom anion. The nbdm species can best be described as two $-C(CN)_2$ moieties bonding to the nitrogen atom of a central nitroso moiety. The anion is close to planar, with each of the dicyanomethanide moieties bent by 6° from the plane formed by the nitroso group and two methanide carbons [C(1)−(N(1)═O(1)]−C(1)† in Figure 1). As is common with polynitrile anions, the near-planar nature of the species and the presence of three resonance structures are indicative of a highly delocalized electronic structure (Scheme 2). The nbdm anion is structurally similar to 1,1,3,3-tetracyanopropane, the 1,1,2,3,3-pentacyanopropenide anion,[45] and the 1,1,3,3-tetracyano-2-oxopropane-1,3-diide dianion.[46]

Scheme 2. Resonance Structures of the nbdm Anion

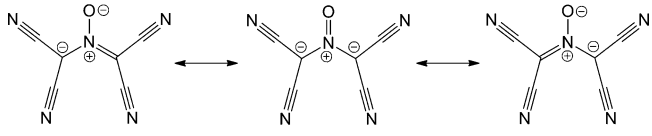

While a molecule of water can readily be added to one nitrile group of the dcnm anion to form the ccnm species,[23c] preliminary experiments during the synthesis of the ccnom anion indicated it could not be synthesized by an analogous route using a dcnom precursor (Scheme 3). This result is not surprising, as it has been shown that the adjacent functional groups of the methanide group may alter the electronic structure of the anion, lowering the reactivity of a nitrile group toward nucleophilic attack.[23c] Therefore, an alternative approach was adopted in which the nitroso group of ccnm was oxidized using Ce^{IV} to give a nitro group, similar to the approach previously used to form dcnom.[22c] After Na(ccnm) was treated with $(NH_4)_2[Ce(NO_3)_6]$ in an acetic acid/water

dx.doi.org/10.1021/cg500051m | Cryst. Growth Des. 2014, 14, 1922−1932

Scheme 3. Alternative Synthetic Route for the Synthesis of the ccnom Anion from a dcnm Precursor

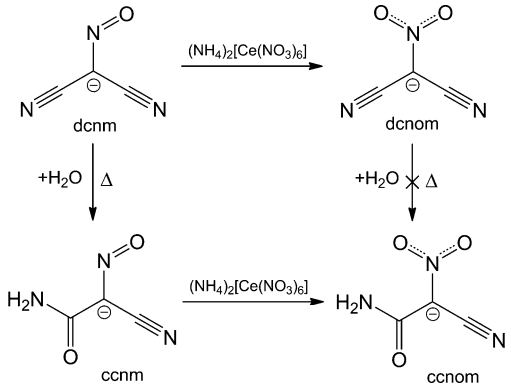

solution, $Ag(NO_3)$ was added to the reaction solution resulting in the formation of a light orange precipitate, which was recrystallized from water to give crystals of Ag(ccnom) (**5**).[47] A metathesis reaction of this product with $(Me_4N)Cl$ yielded (Me_4N)(ccnom), which crystallized from a methanol/diethyl ether solution stored at −18 °C.

Crystal Structures of Organic Salts. The crystal packing of the organic salts examined in this study can be divided into two distinct categories: systems that contain anions without hydrogen-bonding functionalities that form separated columns of anions and cations, namely (Me_4N)(dcnm) (**1**), (Me_4N)(dcnom) (**2**), and (Me_4N)(nbdm) (**3**), and systems that have anions with carbamoyl functionalities in which hydrogen bonding is the dominant supramolecular interaction, namely, (Me_4N)(ccnm) (**4**) and (Me_4N)(ccnom) (**6**). Tetramethylammonium was selected as the counter-cation for all of the salts as it is unlikely to participate in competing hydrogen bonding or $\pi-\pi$ stacking interactions and does not have a significantly delocalized charge or low symmetry, which could result in the formation of a room temperature IL.[17g]

Methanide Anions with Columnar Stacking in Crystal Packing. (Me_4N)(dcnm) (**1**) crystallizes in the monoclinic space group $P2_1/m$, with one formula unit contained in the asymmetric unit (Figure S1 of the Supporting Information). The anion and a portion of the tetramethylammonium cation (C5−N4−C6) lie on a crystallographic mirror plane. The nitroso group of the dcnm anion is disordered over two positions (69/31 occupancy), suggesting that the anion exists in two possible orientations on the same mirror plane that are nearly indistinguishable as the nitrile and methanide moieties were satisfactorily modeled in a single orientation. Therefore, for the purposes of the quantum chemical calculations the dcnm anion is placed in the highest occupancy position at full occupancy.

(Me_4N)(nbdm) (**3**) crystallizes in the monoclinic space group $C2/c$, with half of the formula unit in the asymmetric unit and a mirror plane passing through the nitroso group of the nbdm anion and the nitrogen center of the Me_4N^+ cation (Figure 1).

The crystal packings of both (Me_4N)(dcnm) (**1**) and (Me_4N)(nbdm) (**3**) contain columns of stacked anions that are well-separated from adjacent anion columns by Me_4N^+ counter-cation columns (Figure 2). In both systems, the anions stack with alternating, antiparallel orientations in respect to the immediately adjacent anions in the column. While the direction of stacking is perpendicular to the plane of the dcnm anion in

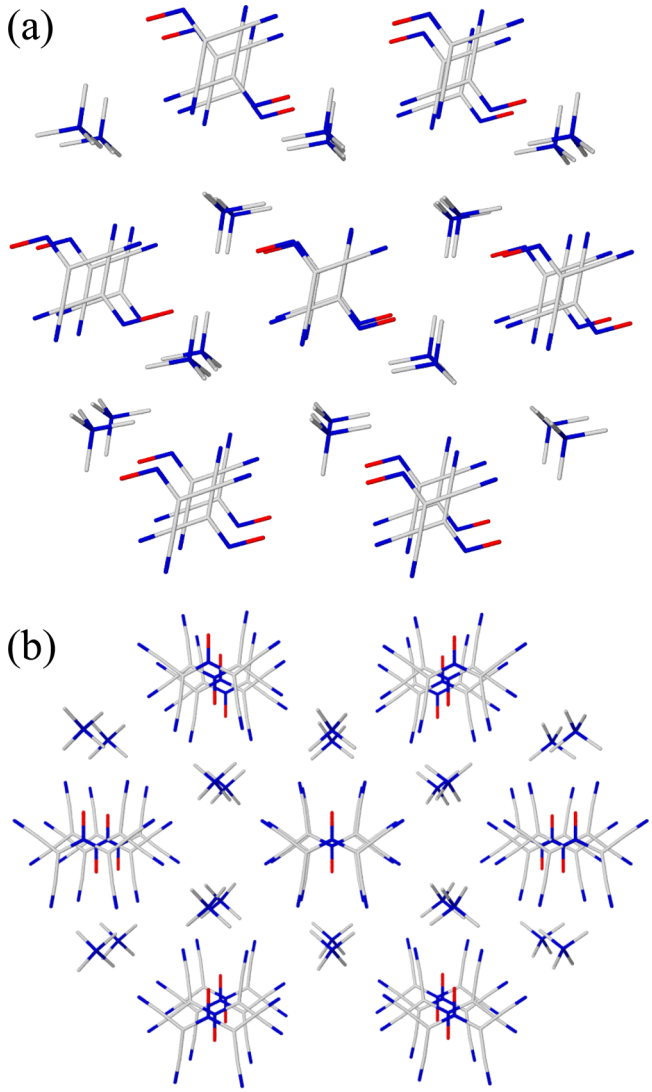

Figure 2. Columns of anions in the crystal structures of (a) (Me_4N)(dcnm) (**1**) viewed down the *a* axis and (b) (Me_4N)(nbdm) (**3**) viewed down the *c* axis. Hydrogen atoms omitted for clarity.

the crystal structure of **1**, the plane of the nbdm anion is slightly canted relative to the direction of the column in **3**, although the anions remain parallel to each other (Figure 3). The interplanar spacing of anions in the crystal structure **3** is shorter than in **1** by 0.14 Å, which could be indicative of a stronger interanionic interaction (see below).

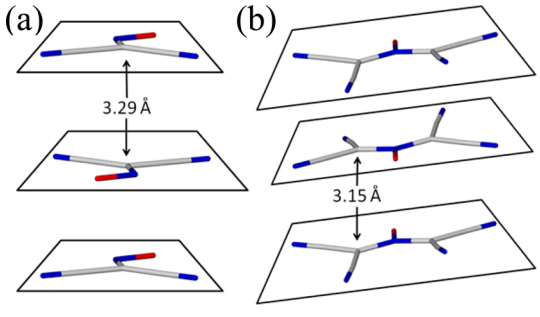

Figure 3. The interplanar spacing between the stacking anions in (a) **1** and (b) **3**.

dx.doi.org/10.1021/cg500051m | *Cryst. Growth Des.* 2014, 14, 1922−1932

While the crystal structure of $(Me_4N)(dcnom)$ (**2**) contains the same anion stacking motif observed in **1** and **3** (Figure 4a),

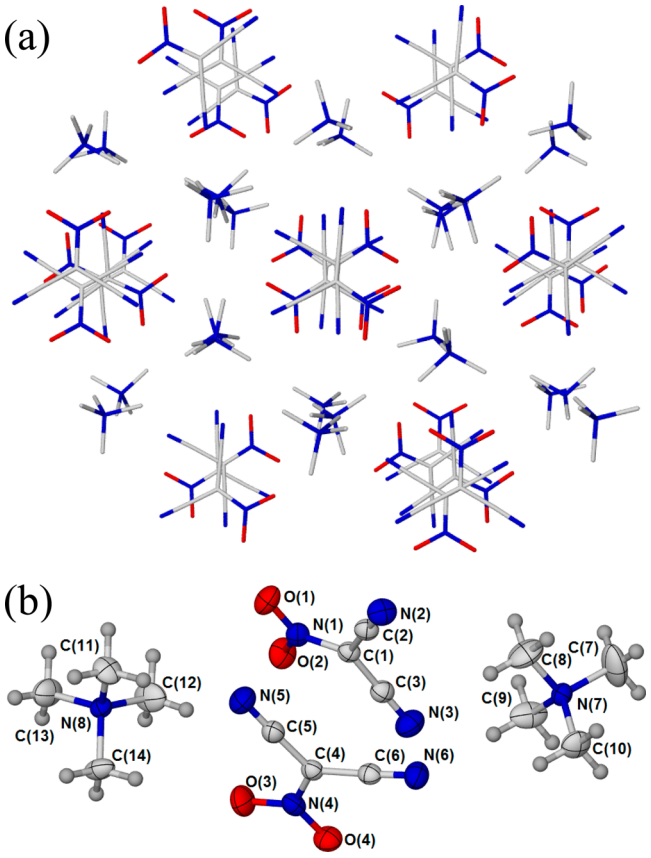

Figure 4. (a) Columns of anions in the crystal structure of $(Me_4N)(dcnom)$ (**2**). Hydrogen atoms omitted for clarity. (b) The asymmetric unit in the crystal structure of **2**. Ellipsoids shown at 50% probability.

there is a difference in how the dcnom species is arranged in the anion column. The tetramethylammonium salt of the dcnom anion crystallizes in the space group $P2_1/c$, with two unique formula units in the asymmetric unit (Figure 4b). The anion columns contain two unique dimers of antiparallel dcnom anions, with interplanar distances of 3.29 and 3.30 Å. These dimers are then canted by 17° relative to each other in the column (Figure 5). While it is not possible to measure the distance between the planes of canted anions as they intercept, the distance between the methanide carbon atoms is 3.37 Å.

Methanide Anions with Hydrogen Bonding in the Crystal Packing. The crystal structure of $(Me_4N)(ccnm)$ (**4**) was first reported in a study detailing nucleophilic addition of water to the dcnm anion[23c] and further described in an investigation into the physical properties of salts of the ccnm anion.[48] In brief, hydrogen bonding between the carbamoyl groups of two ccnm anions gives an $R_2^2(8)$ amide synthon, resulting in the formation of dimers (Figure 6). These dimers then form a very loosely associated 2D sheet, facilitated by the hydrogen bonding between an N−H moiety of an amide group of the ccnm anion to the nitroso group of an adjacent anion (see ref 48 for further details). It is important to note that there are no interactions between the ccnm anions between anionic layers, with Me_4N^+ cations occupying the interlayer space.

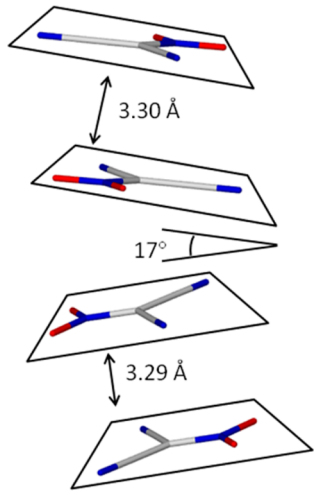

Figure 5. The canted columns of dcnom anion dimers in the crystal structure of **2**.

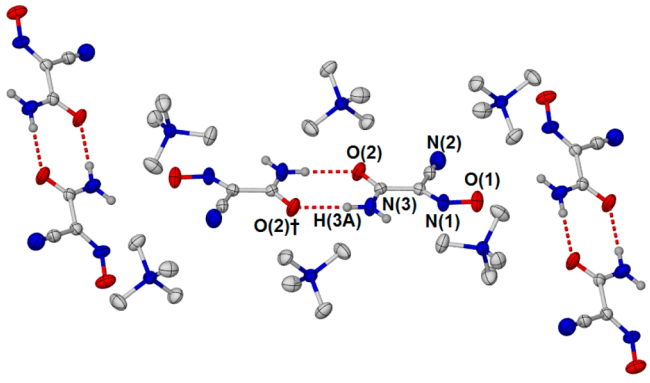

Figure 6. Hydrogen bonding in the crystal structure of (Me_4N)-(ccnm) (**4**). Symmetry element used: † = 1 − *x*, 1 − *y*, 1 − *z*. Ellipsoids shown at 50% probability, hydrogen atoms of Me_4N^+ countercation omitted for clarity. Selected interatomic distances (Å) and angles (deg): N(1)−O(1), 1.293(2); N(1)−C(1), 1.333(3); N(3)···O(2)†, 2.896(2); N(3)−H(3A)···O(2)†, 174.5.

$(Me_4N)(ccnom)$ (**6**) crystallizes in the space group $P2_1/n$, with one formula unit contained in the unit cell. The NH_2 of the carbamoyl group acts as a hydrogen bond donor to the nitrile group of one adjacent anion and the oxygen atom of the carbamoyl group of another anion, facilitating the formation of a 1D hydrogen-bonded chain. This also results in two distinct hydrogen bonding motifs: an $R_2^2(8)$ amide synthon and an $R_2^2(16)$ synthon, which consists of four ccnom anions (Figure 7a). Similar motifs have been observed in the 1D hydrogen-bonded chains of the cdm anion.[26d] There is no columnar stacking of anions between the hydrogen-bonded chains (Figure 7b).

Quantum Chemical Calculations of Anion−Anion Interactions. Clusters containing one, two, and three ion pairs of functionalized methanide anions with tetramethylammonium counter-cations were investigated using ab initio methods in order to further study their electronic structure and packing. It was found that the optimized cluster geometries of dcnm, dcnom, and nbdm anions (Table 1) packed into columns in a similar way to that observed in the X-ray crystal structures. These anions do not have hydrogen atoms, thus preventing the formation of hydrogen bonds. Instead these anions appear to engage in strong $\pi-\pi$ stacking interactions.

dx.doi.org/10.1021/cg500051m | *Cryst. Growth Des.* 2014, 14, 1922−1932

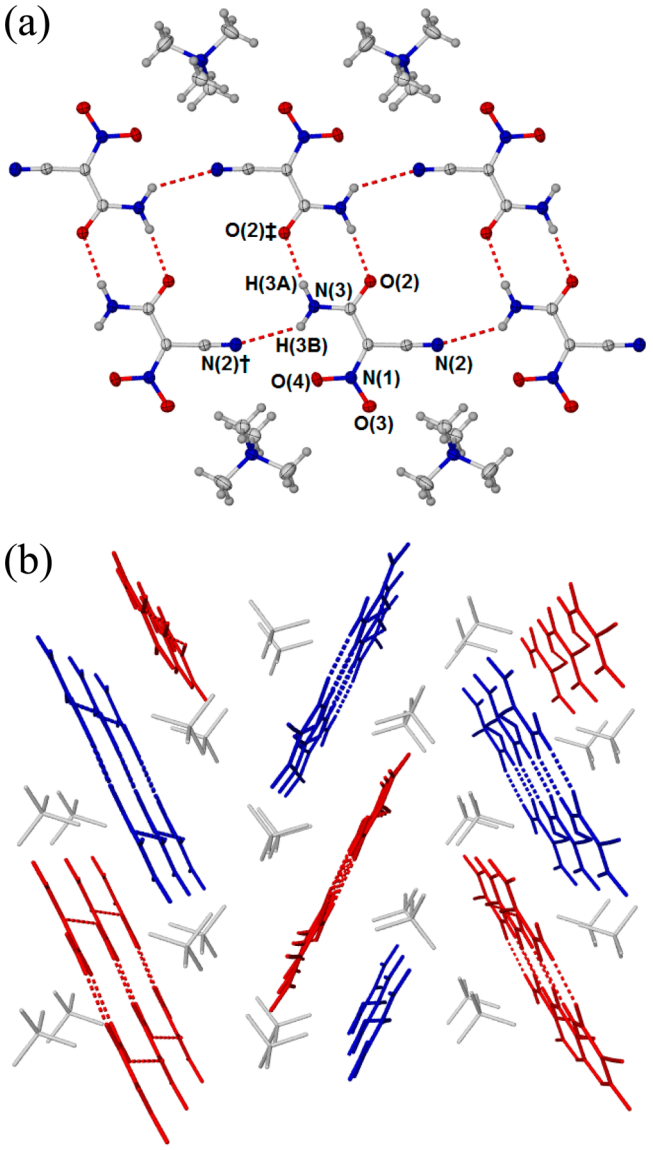

Figure 7. (a) Hydrogen-bonded 1D chains of ccnom anions in the crystal structure of (Me_4N)(ccnom) (**6**). Symmetry elements used: † = 1 + *x*, *y*, *z*; ‡ = 1 − *x*, −*y*, 1 − *z*. Ellipsoids shown at 50% probability. Intramolecular hydrogen bonding not shown for clarity. Hydrogen bond lengths (Å) and angles (deg): N(3)···N(2)†, 3.298(2); N(3)−H(3B)···N(2)†, 135.0; N(3)···O(2)‡, 2.913(2); N(3)−H(3A)···O(2)‡, 173.4; N(3)···O(4), 2.685(2); N(3)−H(3B)···O(4), 129.5. (b) The packing of hydrogen-bonded 1D chains of ccnom anions in **6**, alternately colored in red and blue for clarity. Hydrogen atoms of Me_4N^+ counter-cations (white) omitted for clarity.

Table 2 shows the interplanar distances between two and three ion pair stacks of dcnm, dcnom, and nbdm anions as well as the hydrogen bond distances in ion pair clusters of ccnm. Quantum chemical calculations were not performed on **6**, as the extensive strong hydrogen bonding did not allow for a small representative fraction of the extended crystal structure to be successfully optimized for further energetic analysis at a higher level of theory.

When the anions are modeled in these isolated systems, some deviation from planarity is seen, and the interanionic distances in the columns are smaller than those measured in the crystal structure. However, the calculated values do show agreement with the trends in the experimentally measured values. Calculated distances between the nbdm anions are 0.17 Å smaller than those between the dcnm anions for the two-ion pair cluster, compared with a difference of 0.14 Å, as measured from the X-ray crystal structures, indicating there is a high degree of correlation between the two results. Calculated interanionic distances in the dcnom anion stack are similarly shorter than the measured values for the antiparallel pairs of anions and close in value to the dcnm planar distance. It is expected that the optimized geometries produce shorter interionic distances due to neglect of the field created by surrounding ions in the crystal structure.

Table 1 shows the highest occupied molecular orbital (HOMO) of one, two, and three ion-pair clusters of organic salts **1**, **2**, and **3**. It is seen that significant overlap occurs between the electron densities on the anion species of dcnm, dcnom, and nbdm in a two ion-pair cluster. When three ion-pair clusters are considered the most overlap between the three anions is seen for nbdm. The bonding nature of the HOMOs indicates that there exists a $\pi-\pi$ interaction between the anions as one would observe in the case of the benzene dimer (for more detail on HOMO energies for each cluster see the Supporting Information). The nonplanar packing for the dcnom anion causes the interaction in the HOMO in the three ion-pair cluster to be mainly confined over two of the anions.

The stabilization effects of the $\pi-\pi$ stacking interactions of the anions for **1**, **2**, and **3**, and the hydrogen-bonding interactions in the ccnm dimer in **4** were calculated using FMO3-MP2 with the TZVPP basis set,[41] with the relative interaction energies of the clusters with respect to the corresponding ion pair shown in Table 2. The relative interaction energies calculated using eq 1 mainly recover the energetic effect that the anion stacking imposes on the optimized clusters in **1**, **2**, and **3**, whereas in the clusters of **4**, the hydrogen bonding effect is quantified. This Table also shows the Hartree−Fock (HF) relative interaction energies as an indication of the level of Coulomb and induction interactions in the clusters. From Table 2, it is clear that the planar stacking seen in **1**, **2**, and **3** imparts a large stabilization effect at the FMO3-MP2 level of theory, while stabilization is also seen due to hydrogen bonding in **4**, with the π stacking causing a much larger stabilization effect in **1**, **2** and **3** than hydrogen bonding in **4**. In systems **1**, **2**, and **3**, the addition of a second anion to these species lowers the relative energy of the system by 30.6 kJ mol^{-1} for **1**, 62.1 kJ mol^{-1} for **2**, and 68.6 kJ mol^{-1} for **3**. As predicted, the closer positioning of the nbdm anions and linear columns in **3** cause the greatest overlap of molecular orbitals and, hence, the greatest stabilization effect. The addition of a third ion pair to these systems imparts additional stability with electron density shared over three anions. The stabilization imparted to each cluster is 52.4 kJ mol^{-1} for **1**, 75.2 kJ mol^{-1} for **2**, and 83.4 kJ mol^{-1} for **3**. The interaction energies per ion pair are also expected to increase with an increasing number of ions in the cluster, due to many-body effects, especially nonadditive induction interactions and electron-density driven dispersion interactions.[49] Previously, we showed that for archetypical ionic liquids such as $(Me_4N)(BF_4)$ and $(C_1mim)(BF_4)$, the gain in interaction energy per ion pair (as calculated at the MP2 level of theory) was about 60 kJ mol^{-1} between one and two ion-paired complexes.[41] Further increase in the number of ion pairs to four in the cluster led to an increase in relative interaction energy per ion pair of 75 and 87 kJ mol^{-1} in $(Me_4N)(BF_4)$ and $(C_1mim)(BF_4)$, respectively.

dx.doi.org/10.1021/cg500051m | *Cryst. Growth Des.* 2014, 14, 1922−1932

Table 1. Highest Occupied Molecular Orbital (HOMO) of One, Two, And Three Ion-Pair Clusters of Salts 1, 2, and 3 As Calculated at the M06-2X/cc-pVDZ Level of Theory Using the CPCM Model with Ethanol As Solvent

Ion pairs	(Me_4N)(dcnm) (**1**)	(Me_4N)(dcnom) (**2**)	(Me_4N)(nbdm) (**3**)
1	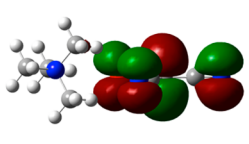	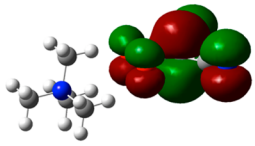	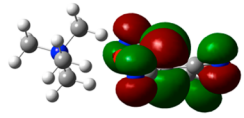
2	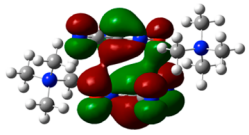	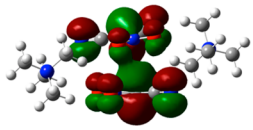	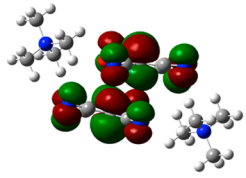
3	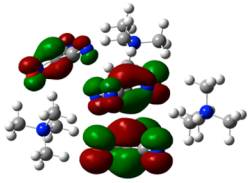	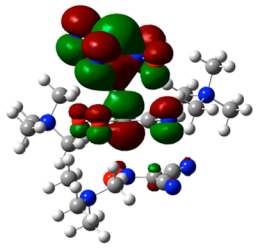	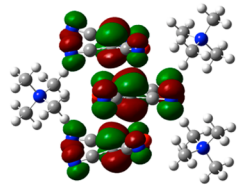

Table 2. Relative Interaction Energies (ΔE_{Int} in kJ mol^{-1}) of and Distances between Two Anions (R in Å) in One, Two, and Three Ion-Paired Clusters of 1, 2, 3, and 4 at the FMO3-MP2/TZVPP//M06-2X/cc-pVDZ Level of Theory[a]

	ΔE_{Int} (kJ mol^{-1})			R (Å)	
salt	1 IP	2 IP	3 IP	2IP	3IP
(Me_4N)(dcnm) (**1**)	0	−30.6 (4.6)	−52.4 (−2.9)	3.12	2.90
					3.25
(Me_4N)(dcnom) (**2**)	0	−62.1 (−20.7)	−75.2 (−15.6)	3.09	3.10
					3.57
(Me_4N)(nbdm) (**3**)	0	−68.6 (−6.9)	−83.4 (1.3)	2.95	3.03
					3.03
(Me_4N)(ccnm) (**4**)	0	−14.7 (−4.8)	12.2 (14.7)	2.90 (N···O═C)	2.87 (N···O═C)
					2.94 (N···O═C)
					2.78 (N···O═N)

[a]Numbers in brackets show the Hartree−Fock (HF) relative interaction energies.

On the basis of these data, it becomes obvious that the stabilization energies of the three ion-pair clusters with stacking between anions are similar to those arising from four ion pairs in archetypical ionic liquids.

Analysis of pairwise interactions calculated as the difference between total electronic energies of a two-fragment system, and those of individual fragments reveals that although the overall anion−anion interaction is positive due to the electrostatic repulsion, the dispersion significantly reduces the repulsion. For example, in 3 ion-paired clusters, each of the two direct anion−anion interactions shows a stabilizing dispersion component of between 36 (structure **2**) and 105 (structure **3**) kJ mol^{-1}. For comparison, cation−cation interactions as well as interactions between anions not in direct contact do not exhibit any appreciable (usually <1 kJ mol^{-1}) dispersion contribution. The analogous direct cation−anion interaction is between 27 (structure **2**) and 30 (structure **3**) kJ mol^{-1} on average, depending on the salt. It has to be noted that these interionic interactions were calculated without accounting for basis set superposition errors, which are expected to be of similar magnitude for interionic interactions in direct contact, thus not affecting the trends discussed above.

In system **4**, hydrogen bonding is the primary interaction between anions and the relative energies of the two ion-pair system quantify the stabilization effect of this interaction at 14.7 kJ mol^{-1} with respect to the reference one ion-pair system. Addition of a third ccnm anion to form the −NH−H···O═N− hydrogen bond, similar to that observed in the crystal structure, did not result in additional stabilization, with the system becoming slightly less stable by a few kJ mol^{-1}. The overall relative interaction energy was found to be positive, +12.2 kJ mol^{-1}, as calculated at the FMO3-MP2 level of theory. This finding is not surprising, as the planar arrangement of the three anions viewed in isolation is not energetically their most stable conformation, indicating that the additional hydrogen bond does not provide additional stability to the crystal structure.

dx.doi.org/10.1021/cg500051m | Cryst. Growth Des. 2014, 14, 1922−1932

Since the structure was optimized in the presence of a solvent field, it is suggested that the surrounding ions play a vital role in stabilizing this type of arrangement, thus resulting in a slightly positive number for the gas-phase relative interaction energy. The dispersion component from the direct anion−anion interactions was estimated as described above and was found to be only 19 kJ mol^{-1} on average compared with that of an averaged 29 kJ mol^{-1} from analogous cation−anion interactions, indicating the minor role of anion−anion interactions on the stability of this cluster. The difference between the −NH−H···O═N− hydrogen bond length observed in the crystal structure and that predicted in the theoretical calculations can be attributed to the fact that no additional restraints were applied during geometry optimization, so the additional hydrogen-bonding interactions for the third anion in the system are not taken into consideration in the model.

The HF contributions to the relative interaction energies are also shown in Table 2. These values show the contribution of Coulomb and induction interactions in the clusters studied. In the archetypical ionic liquids $(Me_4N)(BF_4)$ and $(C_1mim)(BF_4)$, despite similar MP2 stabilization energies (see above), the effect of dispersion measured as the difference between the MP2 and HF relative interaction energies is rather small, about 13 kJ mol^{-1} between one and two ion-paired complexes, increasing to 30 and 20 kJ mol^{-1} for four ion pair clusters of $(Me_4N)(BF_4)$ and $(C_1mim)(BF_4)$, respectively.[41] In system **4**, similar results are seen: only a dispersion contribution of 10 kJ mol^{-1} going to the two ion pair system and approximately 3 kJ mol^{-1} going to the three ion pair system. Therefore, in its crystal form, **4** shows similar contributions from dispersion as a typical ionic liquid. However, from Table 2, it is clear that the dispersion contribution to the relative interaction energy of the stacked anions in **1**, **2**, and **3** is much greater, up to around 85 kJ mol^{-1} going from one to three ion pairs for **3**. For the **1** and **3** systems, the HF relative interaction energy is close to zero and therefore it is clear that dispersion interactions are primarily responsible for the stabilization seen between the stacked π systems in these clusters.

In conclusion, the $\pi-\pi$ stacking in **1**, **2**, and **3** is clearly dominated by dispersion-driven interactions between electron densities of the anions, with Coulomb and induction forces causing a slight destabilization in some instances. System **4** shows a similar trend for the dispersion component of interaction energy to that found in archetypical ionic liquids such as $(Me_4N)(BF_4)$ and $(C_1mim)(BF_4)$.[41]

Unfortunately, DSC and melting point measurements on these salts could not be compared with theoretically predicted trends in stability of **1**, **2**, **3**, and **4**. Unlike their ionic liquid pyrollidinium salt analogues, both (Me_4N)(dcnm) (**1**) and (Me_4N)(ccnm) (**4**) decompose before melting at temperatures below 200 and 150 °C, respectively.[17g,48] For this study, the melting point of (Me_4N)(dcnom) (**2**) was determined by DSC measurement to be 202 °C (Figure S2 of the Supporting Information). While the thermal properties of these salts did not assist in examining the trends predicted by theoretical calculations, the fact that these materials decompose before melting or have a high melting point, viewed in conjunction with previous reports that these anions are easily incorporated into ionic liquids with bulky countercations, suggests that the presence of anion−anion interactions in the crystal structure leads to a more thermally stable solid phase.

CONCLUSION

In addition to reporting the first syntheses of two novel methanide anions, nitroso-*N*,*N*-bis(dicyanomethanide) (nbdm) and carbamoylcyanonitromethanide (ccnom), we have demonstrated that highly unusual interanion $\pi-\pi$ stacking occurs in the functionalized polynitrile methanide family. The crystal structures of the tetramethylammonium salts of dcnm (**1**), dcnom (**2**), and nbdm (**3**) reveal the cyanomethanide species pack in a columnar structure, indicating there is an attractive intermolecular interaction between the anions. In the crystal structures of the related organic salts (Me_4N)(ccnm) (**4**) and (Me_4N)(ccnom) (**6**), the presence of a carbamoyl functional group on the anion results in hydrogen-bonding interactions becoming the predominant intermolecular anion−anion interaction. A high level of ab initio theory was used to model one, two, and three ion pairs of **1**−**4**, with a strong correlation observed between the experimental crystal structures and the computational models. For **1**−**3**, increasing the number of ion pairs resulted in a greater stabilization of the systems compared to archetypical ionic liquids, with dispersion-driven interaction dominating the $\pi-\pi$ interactions between the anions. This greater understanding of the unusual supramolecular interactions of this family of anions will aid in tailoring their properties for ionic liquids and ionic plastic crystals and possibly open a pathway to future application in organic electronics.

ASSOCIATED CONTENT

Supporting Information

Figure of (Me_4N)(dcnm) (**1**) with anion disorder, DSC measurement of (Me_4N)(dcnom) (**2**), tables of optimized structures and FMO3-MP2/TZVPP//M06-2X/cc-pVDZ energies and basis set superposition errors (BSSE) of ion pairs, and Gaussian archive entries of optimized structures. This material is available free of charge via the Internet at http://pubs.acs.org.

AUTHOR INFORMATION

Corresponding Authors

*E-mail: katya.pas@monash.edu.
*E-mail: stuart.batten@monash.edu.

Author Contributions

The manuscript was written through contributions of all authors. All authors have given approval to the final version of the manuscript.

Notes

The authors declare no competing financial interest.

ACKNOWLEDGMENTS

We thank the Australian Research Council for funding Discovery grants (S.R.B., G.B.D., D.R.T., and E.I.I.), ARC Future Fellowships (E.I.I., D.R.T., and S.R.B.), and a Discovery Early Career Researcher Award (DECRA) (A.S.R.C). D.R.T. and A.S.R.C. also thank Australian Institute of Nuclear Science and Engineering for financial support. We gratefully acknowledge generous allocations of computing time from the National Facility of the National Computational Infrastructure (Canberra, Australia) and the Monash Campus Cluster at the *e*Research Centre of Monash University, Australia.

■ ABBREVIATIONS

ccnom, carbamoylcyanonitromethanide; ccnm, carbamoylcyanonitrosomethanide; cnnom, cyanonitronitrosomethanide; cdnom, cyanodinitromethanide; dcnom, dicyanonitromethanide; dcnm, dicyanonitrosomethanide; nbdm, nitroso-*N*,*N*-bis(dicyanomethanide)

■ REFERENCES

(1) (a) Nelyubina, Y. V.; Antipin, M. Y.; Lyssenko, K. A. *Russ. Chem. Rev.* **2010**, *79*, 167. (b) Dance, I.; Scudder, M. *Chem.—Eur. J.* **1996**, *2*, 481−486.

(2) Groenewald, F.; Esterhuysen, C.; Dillen, J. *Theor. Chem. Acc.* **2012**, *131*, 1−12.

(3) Nelyubina, Y. V.; Lyssenko, K. A.; Golovanov, D. G.; Antipin, M. Y. *CrystEngComm* **2007**, *9*, 991−996.

(4) Konarev, D. V.; Zorina, L. V.; Ishikawa, M.; Khasanov, S. S.; Otsuka, A.; Yamochi, H.; Saito, G.; Lyubovskaya, R. N. *Cryst. Growth Des.* **2013**, *13*, 4930−4939.

(5) Nelyubina, Y. V.; Antipin, M. Y.; Lyssenko, K. A. *J. Phys. Chem. A* **2007**, *111*, 1091−1095.

(6) Nelyubina, Y. V.; Lyssenko, K. A.; Kotov, V. Y.; Antipin, M. Y. *J. Phys. Chem. A* **2008**, *112*, 8790−8796.

(7) (a) Mathew, S.; Paul, G.; Shivasankar, K.; Choudhury, A.; Rao, C. N. R. *J. Mol. Struct.* **2002**, *641*, 263−279. (b) Braga, D.; Bazzi, C.; Grepioni, F.; J. Novoa, J. *New J. Chem.* **1999**, *23*, 577−579. (c) Braga, D.; Maini, L.; Polito, M.; Grepioni, F. Hydrogen Bonding Interactions Between Ions: A Powerful Tool in Molecular Crystal Engineering. In *Supramolecular Assembly via Hydrogen Bonds II*, Mingos, D. M., Ed. Springer: Berlin, 2004; Vol. *111*, pp 1−32. (d) Mata, I.; Alkorta, I.; Molins, E.; Espinosa, E. *Chem. Phys. Lett.* **2013**, *555*, 106−109. (e) Mata, I.; Alkorta, I.; Molins, E.; Espinosa, E. *ChemPhysChem* **2012**, *13*, 1421−1424.

(8) (a) Kaim, W.; Moscherosch, M. *Coord. Chem. Rev.* **1994**, *129*, 157−193. (b) Ashwell, G. J. *Phys. Status Solidi B* **1978**, *86*, 705−715. (c) Huang, J.; Kingsbury, S.; Kertesz, M. *Phys. Chem. Chem. Phys.* **2008**, *10*, 2625−2635.

(9) Tanaka, J.; Tanaka, M.; Kawai, T.; Takabe, T.; Maki, O. *Bull. Chem. Soc. Jpn.* **1976**, *49*, 2358−2373.

(10) (a) McQueen, A. E. D.; Blake, A. J.; Stephenson, T. A.; Schroder, M.; Yellowlees, L. J. *J. Chem. Soc., Chem. Commun.* **1988**, *0*, 1533−1535. (b) Braunwarth, H.; Huttner, G.; Zsolnai, L. *J. Organomet. Chem.* **1989**, *372*, C23−C28. (c) Humphrey, D. G.; Fallon, G. D.; Murray, K. S. *J. Chem. Soc., Chem. Commun.* **1988**, *0*, 1356−1358.

(11) (a) Bock, H.; Näther, C.; Ruppert, K. *Z. Anorg. Allg. Chem.* **1992**, *614*, 109−114. (b) Bock, H.; Ruppert, K. *Inorg. Chem.* **1992**, *31*, 5094−5099.

(12) (a) Filhol, A.; Zeyen, C. M. E.; Chenavas, P.; Gaultier, J.; Delhaes, P. *Acta Crystallogr., Sect. B: Struct. Sci.* **1980**, *36*, 2719−2726. (b) Chen, Y.-C.; Wang, P.-F.; Liu, G.-X.; Xu, H.; Ren, X.-M.; Song, Y.; Ni, Z.-P. *J. Phys. Chem. Solids* **2008**, *69*, 2445−2452.

(13) (a) Clemenson, P. I. *Coord. Chem. Rev.* **1990**, *106*, 171−203. (b) Ni, C.; Zheng, Y.; Le, X. *J. Coord. Chem.* **2006**, *59*, 1173−1182. (c) Ni, C.; Li, Y.; Meng, Q. *J. Coord. Chem.* **2005**, *58*, 759−766. (d) Ni, C.; Li, Y.; Ni, Z.; Meng, Q. *J. Coord. Chem.* **2004**, *57*, 1321−1328. (e) Lewis, G. R.; Dance, I. *J. Chem. Soc., Dalton Trans.* **2000**, 3176−3185. (f) Ren, X. M.; Okudera, H.; Kremer, R. K.; Song, Y.; He, C.; Meng, Q. J.; Wu, P. H. *Inorg. Chem.* **2004**, *43*, 2569−2576.

(14) (a) Ni, C.; Dang, D.; Song, Y.; Gao, S.; Li, Y.; Ni, Z.; Tian, Z.; Wen, L.; Meng, Q. *Chem. Phys. Lett.* **2004**, *396*, 353−358. (b) Xie, J.; Ren, X.; Song, Y.; Zou, Y.; Meng, Q. *J. Chem. Soc., Dalton Trans.* **2002**, 2868−2872. (c) Ribas, X.; Mas-Torrent, M.; Pérez-Benítez, A.; Dias, J. C.; Alves, H.; Lopes, E. B.; Henriques, R. T.; Molins, E.; Santos, I. C.; Wurst, K.; Foury-Leylekian, P.; Almeida, M.; Veciana, J.; Rovira, C. *Adv. Funct. Mater.* **2005**, *15*, 1023−1035.

(15) (a) Gama, V.; Henriques, R. T.; Bonfait, G.; Pereira, L. C.; Waerenborgh, J. C.; Santos, I. C.; Duarte, M. T.; Cabral, J. M. P.; Almeida, M. *Inorg. Chem.* **1992**, *31*, 2598−2604. (b) Ni, Z.; Ren, X.; Ma, J.; Xie, J.; Ni, C.; Chen, Z.; Meng, Q. *J. Am. Chem. Soc.* **2005**, *127*, 14330−14338.

(16) (a) Turner, D. R.; Chesman, A. S. R.; Murray, K. S.; Deacon, G. B.; Batten, S. R. *Chem. Commun.* **2011**, *47*, 10189−10210. (b) Brand, H.; Mayer, P.; Polborn, K.; Schulz, A.; Weigand, J. J. *J. Am. Chem. Soc.* **2005**, *127*, 1360−1361. (c) Brand, H.; Mayer, P.; Schulz, A.; Weigand, J. J. *Angew. Chem., Int. Ed.* **2005**, *44*, 3929−3932. (d) Brand, H.; Schulz, A.; Villinger, A. *Z. Anorg. Allg. Chem.* **2007**, *633*, 22−35.

(17) (a) Emel'yanenko, V. N.; Zaitsau, D. H.; Verevkin, S. P.; Heintz, A.; Voß, K.; Schulz, A. *J. Phys. Chem. B* **2011**, *115*, 11712−11717. (b) Conceicao, L. J. A.; Bogel-Lukasik, E.; Bogel-Lukasik, R. *RSC Adv.* **2012**, *2*, 1846−1855. (c) Penalber, C. Y.; Grenoble, Z.; Baker, G. A.; Baldelli, S. *Phys. Chem. Chem. Phys.* **2012**, *14*, 5122−5131. (d) Forsyth, S. A.; Batten, S. R.; Dai, Q.; MacFarlane, D. R. *Aust. J. Chem.* **2004**, *57*, 121−124. (e) Chesman, A. S. R.; Yang, M.; Spiccia, N. D.; Deacon, G. B.; Batten, S. R.; Mudring, A.-V. *Chem.—Eur. J.* **2012**, *18*, 9580−9589. (f) Chesman, A. S. R.; Yang, M.; Mallick, B.; Ross, T. M.; Gass, I. A.; Deacon, G. B.; Batten, S. R.; Mudring, A.-V. *Chem. Commun.* **2012**, *48*, 124−126. (g) Janikowski, J.; Razali, M. R.; Batten, S. R.; MacFarlane, D. R.; Pringle, J. M. *ChemPlusChem* **2012**, *77*, 1039−1045. (h) Brand, H.; Liebman, J. F.; Schulz, A.; Mayer, P.; Villinger, A. *Eur. J. Inorg. Chem.* **2006**, *2006*, 4294−4308.

(18) (a) Wang, P.; Wenger, B.; Humphry-Baker, R.; Moser, J.-E.; Teuscher, J.; Kantlehner, W.; Mezger, J.; Stoyanov, E. V.; Zakeeruddin, S. M.; Grätzel, M. *J. Am. Chem. Soc.* **2005**, *127*, 6850−6856. (b) Wang, P.; Zakeeruddin, S. M.; Grätzel, M.; Kantlehner, W.; Mezger, J.; Stoyanov, E. V.; Scherr, O. *Appl. Phys. A: Mater. Sci. Process.* **2004**, *79*, 73−77. (c) Marszalek, M.; Fei, Z.; Zhu, D.-R.; Scopelliti, R.; Dyson, P. J.; Zakeeruddin, S. M.; Grätzel, M. *Inorg. Chem.* **2011**, *50*, 11561−11567.

(19) Gerasimchuk, N.; Maher, T.; Durham, P.; Domasevitch, K. V.; Wilking, J.; Mokhir, A. *Inorg. Chem.* **2007**, *46*, 7268−7284.

(20) (a) Murray, K. S. *Aust. J. Chem.* **2009**, *62*, 1081−1101. (b) Batten, S. R.; Murray, K. S. *Coord. Chem. Rev.* **2003**, *246*, 103−130.

(21) Glover, G.; Gerasimchuk, N.; Biagioni, R.; Domasevitch, K. V. *Inorg. Chem.* **2009**, *48*, 2371−2382.

(22) (a) Gao, H.; Zeng, Z.; Twamley, B.; Shreeve, J. M. *Chem.−Eur. J.* **2008**, *14*, 1282−1290. (b) Gao, H.; Joo, Y.-H.; Twamley, B.; Zhou, Z.; Shreeve, J. n. M. *Angew. Chem., Int. Ed.* **2009**, *48*, 2792−2795. (c) Arulsamy, N.; Bohle, D. S.; Doletski, B. G. *Inorg. Chem.* **1999**, *38*, 2709−2715. (d) Wang, R.; Gao, H.; Ye, C.; Twamley, B.; Shreeve, J. M. *Inorg. Chem.* **2007**, *46*, 932−938.

(23) (a) Arulsamy, N.; Bohle, D. S. *J. Org. Chem.* **2000**, *65*, 1139−1143. (b) Hvastijová, M.; Kohout, J.; Buchler, J. W.; Boča, R.; Kožíšek, J.; Jäger, L. *Coord. Chem. Rev.* **1998**, *175*, 17−42. (c) Izgorodina, E. I.; Chesman, A. S. R.; Turner, D. R.; Deacon, G. B.; Batten, S. R. *J. Phys. Chem. B* **2010**, *114*, 16517−16527.

(24) (a) Chesman, A. S. R.; Turner, D. R.; Deacon, G. B.; Batten, S. R. *Chem.−Asian J.* **2009**, *4*, 761−769. (b) Chesman, A. S. R.; Turner, D. R.; Moubaraki, B.; Murray, K. S.; Deacon, G. B.; Batten, S. R. *Aust. J. Chem.* **2009**, *62*, 1137−1141. (c) Chesman, A. S. R.; Turner, D. R.; Moubaraki, B.; Murray, K. S.; Deacon, G. B.; Batten, S. R. *Chem.−Eur. J.* **2009**, *15*, 5203−5207. (d) Chesman, A. S. R.; Turner, D. R.; Moubaraki, B.; Murray, K. S.; Deacon, G. B.; Batten, S. R. *Eur. J. Inorg. Chem.* **2010**, 59−73. (e) Chesman, A. S. R.; Turner, D. R.; Price, D. J.; Moubaraki, B.; Murray, K. S.; Deacon, G. B.; Batten, S. R. *Chem. Commun.* **2007**, 3541−3543. (f) Turner, D. R.; Pek, S. N.; Cashion, J. D.; Moubaraki, B.; Murraya, K. S.; Batten, S. R. *Dalton Trans.* **2008**, 6877−6879. (g) Razali, M. R.; Urbatsch, A.; Langley, S. K.; MacLellan, J. G.; Deacon, G. B.; Moubaraki, B.; Murray, K. S.; Batten, S. R. *Aust. J. Chem.* **2012**, *65*, 918−925. (h) Razali, M. R.; Urbatsch, A.; Deacon, G. B.; Batten, S. R. *Inorg. Chim. Acta* **2013**, *403*, 120−126. (i) Razali, M. R.; Chilton, N. F.; Urbatsch, A.; Moubaraki, B.; Langley, S. K.; Murray, K. S.; Deacon, G. B.; Batten, S. R. *Polyhedron* **2013**, *52*, 797−803. (j) Razali, M. R.; Urbatsch, A.; Deacon, G. B.; Batten, S. R. *Polyhedron* **2013**, *64*, 352−364.

(25) (a) Gewald, K.; Bellmann, P.; Jänsch, H.-J. *Liebigs Ann. Chem.* **1980**, *1980*, 1623−1629. (b) Bland, D. C.; Raudenbush, B. C.; Weinreb, S. M. *Org. Lett.* **2000**, *2*, 4007−4009.

(26) (a) Turner, D. R.; Batten, S. R. *Cryst. Growth Des.* **2010**, *10*, 2501−2508. (b) Turner, D. R.; Pek, S. N.; Batten, S. R. *New J. Chem.* **2008**, *32*, 719−726. (c) Turner, D. R.; MacDonald, R.; Lee, W. T.; Batten, S. R. *CrystEngComm* **2009**, *11*, 298−305. (d) Turner, D. R.; Pek, S. N.; Batten, S. R. *CrystEngComm* **2009**, *11*, 87−93. (e) Turner, D. R.; Edwards, A. J.; Piltz, R. O. *CrystEngComm* **2012**, *14*, 6447−6451. (f) Emerson, A. J.; Edwards, A. J.; Batten, S. R.; Turner, D. R. *CrystEngComm* **2014**, *16*, 1625−1631.
(27) Longo, G. *Gazz. Chim. Ital.* **1931**, *61*, 575−583.
(28) Arulsamy, N.; Bohle, D. S.; Doletski, B. G. *Inorg. Chem.* **1999**, *38*, 2709−2715.
(29) Sheldrick, G. M. *Acta Crystallogr., Sect. A* **2008**, *64*, 112−122.
(30) Barbour, L. J. *J. Supramol. Chem.* **2001**, *1*, 189−191.
(31) Otwinowski, Z.; Minor, W. *Methods in Enzymology*; Academic Press: New York, 1997; Vol. *276*.
(32) *ApexII Bruker AXS Ltd.*; Bruker: Madison, WI, 2005.
(33) Zhao, Y.; Truhlar, D. *Theor. Chem. Acc.* **2008**, *120*, 215−241.
(34) Dunning, J. T. H. *J. Chem. Phys.* **1989**, *90*, 1007−1023.
(35) (a) Barone, V.; Cossi, M. *J. Phys. Chem. A* **1998**, *102*, 1995−2001. (b) Cossi, M.; Rega, N.; Scalmani, G.; Barone, V. *J. Comput. Chem.* **2003**, *24*, 669−681.
(36) Izgorodina, E. I.; Forsyth, M.; MacFarlane, D. R. *Phys. Chem. Chem. Phys.* **2009**, *11*, 2452−2458.
(37) Nakano, T.; Kaminuma, T.; Sato, T.; Fukuzawa, K.; Akiyama, Y.; Uebayasi, M.; Kitaura, K. *Chem. Phys. Lett.* **2002**, *351*, 475−480.
(38) Møller, C.; Plesset, M. S. *Phys. Rev.* **1934**, *46*, 618−622.
(39) Schafer, A.; Huber, C.; Ahlrichs, R. *J. Chem. Phys.* **1994**, *100*, 5829−5835.
(40) (a) Fedorov, D. G.; Ishimura, K.; Ishida, T.; Kitaura, K.; Pulay, P.; Nagase, S. *J. Comput. Chem.* **2007**, *28*, 1476−1484. (b) Fedorov, D. G.; Kitaura, K. *J. Chem. Phys.* **2004**, *120*, 6832−6840.
(41) Izgorodina, E. I.; Rigby, J.; MacFarlane, D. R. *Chem. Commun.* **2012**, *48*, 1493−1495.
(42) Boys, S. F.; Bernardi, F. *Mol. Phys.* **1970**, *19*, 553−566.
(43) Frisch, M. J.; Trucks, G. W.; Schlegel, H. B.; Scuseria, G. E.; Robb, M. A.; Cheeseman, J. R.; Montgomery, J. A.; Jr., Vreven, T.; Kudin, K. N.; Burant, J. C.; Millam, J. M.; Iyengar, S. S.; Tomasi, J.; Barone, V.; Mennucci, B.; Cossi, M.; Scalmani, G.; Rega, N.; Petersson, G. A.; Nakatsuji, H.; Hada, M.; Ehara, M.; Toyota, K.; Fukuda, R.; Hasegawa, J.; Ishida, M.; Nakajima, T.; Honda, Y.; Kitao, O.; Nakai, H.; Klene, M.; Li, X.; Knox, J. E.; Hratchian, H. P.; Cross, J. B.; Bakken, V.; Adamo, C.; Jaramillo, J.; Gomperts, R.; Stratmann, R. E.; Yazyev, O.; Austin, A. J.; Cammi, R.; Pomelli, C.; Ochterski, J. W.; Ayala, P. Y.; Morokuma, K.; Voth, G. A.; Salvador, P.; Dannenberg, J. J.; Zakrzewski, V. G.; Dapprich, S.; Daniels, A. D.; Strain, M. C.; Farkas, O.; Malick, D. K.; Rabuck, A. D.; Raghavachari, K.; Foresman, J. B.; Ortiz, J. V.; Cui, Q.; Baboul, A. G.; Clifford, S.; Cioslowski, J.; Stefanov, B. B.; Liu, A. L.; Piskorz, P.; Komaromi, I.; Martin, R. L.; Fox, D. J.; Keith, T.; Al-Laham, M. A.; Peng, C. Y.; Nanayakkara, A.; Challacombe, M.; Gill, P. M. W.; Johnson, B.; Chen, W.; Wong, M. W.; Gonzalez, C.; Pople, J. A. *GAUSSIAN 09*, revision A.02; Gaussian, Inc.: Wallingford, CT, 2009.
(44) (a) Schmidt, M. W.; Baldridge, K. K.; Boatz, J. A.; Elbert, S. T.; Gordon, M. S.; Jensen, J. H.; Koseki, S.; Matsunaga, N.; Nguyen, K. A.; Su, S.; Windus, T. L.; Dupuis, M.; Montgomery, J. A. *J. Comput. Chem.* **1993**, *14*, 1347−1363. (b) Gordon, M. S.; Schmidt, M. W. Advances in Electronic Structure Theory: GAMESS a decade later. In *Theory and Applications of Computational Chemistry, the First Forty Years*, Dykstra, C. E., Frenking, G., Kim, K. S. Scuseria, G. E., Eds.; Elsevier: Amsterdam, 2005; pp 1167−1189.
(45) Jäger, L.; Wagner, C.; Hanke, W. *J. Mol. Struct.* **2000**, *525*, 107−111.
(46) Atmani, C.; Setifi, F.; Benmansour, S.; Triki, S.; Marchivie, M.; Salaün, J.-Y.; Gómez-García, C. J. *Inorg. Chem. Commun.* **2008**, *11*, 921−924.
(47) The crystal structure of Ag(ccnom) is to be discussed in a future publication.
(48) Janikowski, J.; Razali, M. R.; Forsyth, C. M.; Nairn, K. M.; Batten, S. R.; MacFarlane, D. R.; Pringle, J. M *ChemPlusChem* **2013**, *78*, 486−497.
(49) Izgorodina, E. I. *Phys. Chem. Chem. Phys.* **2011**, *13*, 4189−4207.